EFFECT OF MICROESTRUCTURE OF X-65 IN BIOETHANOL FOR PIPELINES

M.A. Lucio-García [a], J.G. González-Rodríguez [a], S. Serna [a], A. Torres-Islas [b].
a *CIICAP-UAEM, Av. Universidad 1001, Col. Chamilpa, 62209-Cuernavaca, Morelos, México.*
b FCQeI-UAEM, Av. Universidad 1001, Col. Chamilpa, 62209-Cuernavaca, Morelos, México.

ABSTRACT

Fuel grade ethanol, (FGE) is attracted much attention due the increasing demand for fossil fuel alternatives and reducing carbon oxide emissions [1]. Although the occurrence of ethanol SCC thus far has not caused major problems, extensive pipeline transport of ethanol in the future requires sufficient understanding of the phenomenon to resolve this concern. Tensile test employed to study effects of kinetics of X-65 steel. Recent phenomenological studies have identified several constituents that significantly affect corrosion and Stress Corrosion Cracking (SCC) susceptibility in this alternative fuel. Ethanol corrosion-SCC have been the topics of numerous recent evaluations [2-11]. As well steel corrosion in FGE was investigated by electrochemical measurements on electrodes, as polarization curves and electrochemical noise. SCC has been evaluated by slow strain rate testing to evaluate hydrogen embrittlement under cathodic protection, reduction in area and percentage elongation of tensile specimens to asses the degree of embrittlement.

INTRODUCTION

Energy is the backbone of social and economic development of countries, but their production methods are not adequate to ensure the growing demand for sustainably enough; is in this way that the generation of energy from renewable sources, such as biodiesel or bioethanol, which are very promising alternative fuels can reduce economic, political and environmental costs, because the society would cease to depend on fossil fuels. The generation of these biofuels and their use cause corrosion damage in materials during storage, transport and use, and the results have shown that some materials have electrochemical mechanism which is under diffusion control; checking that biofuel is more corrosive than diesel oil, according to the reported information, which is degraded by moisture absorption, oxidation and other contaminants.

EXPERIMENTAL PROCEDURE

Electrochemical measurements

SSRT tests and polarization curves

Cylindrical tensile specimens with a 25 mm gauge length and 2.5 mm gauge diameter were machined. Before testing, the specimens were abraded longitudinally with 600 grade emery paper, degreased and masked. Specimens were subjected to conventional monotonic slow strain rate tensile (SSRT) testing in a solution which

composition of baseline simulate fuel-grade ethanol (SFGE) used in this study based consisted of 98.5% ethanol, 0.5% methanol, 1% water, 32 mg/L NaCl, 56 mg/L acetic acid according ASTM D-4806 [13] at room temperature a strain rate of 1 X $10^{-6}s^{-1}$.
All the tests were done at the open circuit potential. The loss in ductility was assessed in terms of the percentage reduction in area (%R.A.) by using

——— (1)

Where Ai and Af are the initial a final area respectively. Tensile fractured specimens were examined by a JEOL scanning electron microscope (SEM).

Electrochemical techniques employed included potenthiodynamic polarization curves and electrochemical noise measurements. Polarization curves were performed at sweep rate of 1 mV/s using a fully automated AC Gill potentiostat controlled with a desk top computer in the NACE solution and the scanning range was from -1000 to +1000 mV respect to the open circuit potential, E_{corr} Inhibition efficiencies (*E(%)*) were determined from the corrosion current densities calculated by the Tafel extrapolation method according to the following equation

$$E(\%) = \frac{i_i - i_b}{i_i} \text{X } 100 \quad (2)$$

where i_b is the corrosion rate without inhibitor and i_i the corrosion rate in the solution with inhibitor.

Results and Discussion

Electrochemical measurements cyclic potentiodynamic polarization monitoring were used in this work. Polarization tests were carried out using a Gill electrochemical measurement system in a three-electrode electrochemical testing cell. A calomel reference electrode and an auxiliary electrode was graphite. Fig. 1 shows the polarization curves with different percentages of water, which shows that there is no passivation of the polarization curves, as there are only anodic dissolution. The more negative potential corresponding to 1% of water followed by 50% of water, then 5 to 20% of water having the most positive potential of 10% water. With low concentration of water, pit density and pit size increase as the water concentration increases.
Icorr value calculated by Tafel extrapolation more negative is the percentage of 1% water, while the positive value is 20% water.

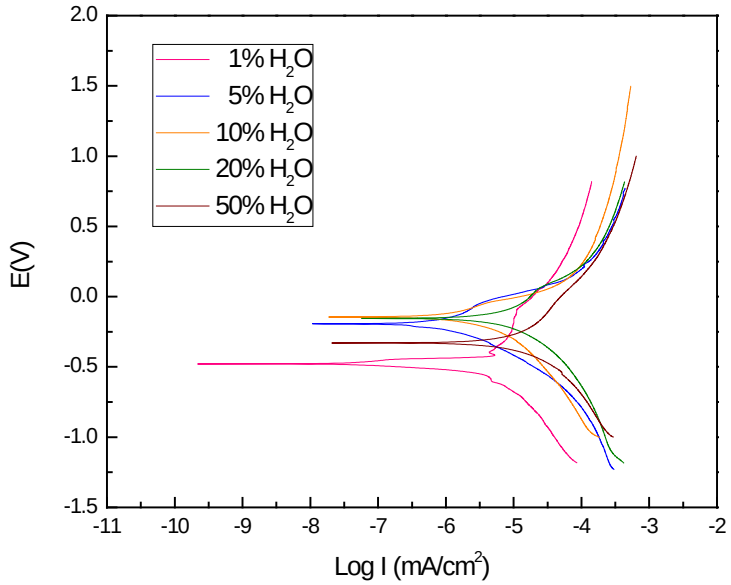

Fig.1 Effect of percent hydrogen on the polarization curves for steel X-65.

Fig. 2 shows the effect of percentage of hydrogen on the susceptibility towards SSC as measured by the percentage reduction in area % R.A. where it can be seen that the most susceptible percentage towards SSC was for 5%. There was a tendency to recover the ductility as the percentage of water increased up, it means, for 10, and 20%.

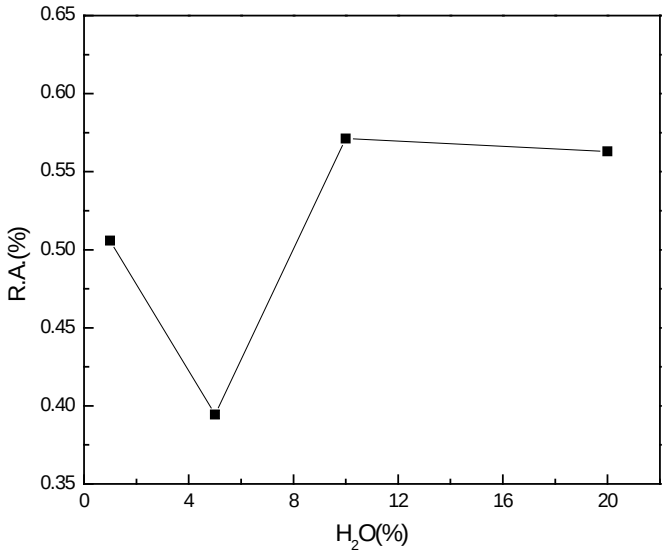

Fig. 2 Effect of percent hydrogen on the percentage reduction in area value for X-65 steel.

For the anodic reaction, the presence of water alters the oxidation reaction on metal.

Conclusions

Steel X-65 were measured in a simulated fuel grade ethanol environment as a function of the fracture mechanics stress-intensity-factor.
For the anodic reaction, the presence of water alters the oxidation reaction on metal. More iron oxide and hydroxide form under these condition. Due to the limited amount of water, the hydroxide may for in such SFGE tends to be unstable and easy to dissociate into oxide form. Corrosion products with multiple oxidation states may be present in the form of oxide.
The purpose of the present study was to understand better the effects of metallurgical factors in bioethanol on X-45 and identified that dissolved oxygen and corrosion potential are the critical factors contributing in pipeline steel, in conjunction with the effect of electrochemical potential on the external SCC in SFGE solutions using the slow strain rate testing (SSRT) technique. However, impurities and additives can promote tendencies toward localized corrosion with low levels of water contamination.

References:

[1] A. Dermibas, Biofuels sources, biofuel policy, biofuel economy and global biofuel.
[2] R.D. Kane, N. Sridhar, M.P. Brongers, J.A. Beavers, A.K. Agrawal, L.J. Klein, Stress
corrosion cracking in fuel ethanol: a recently recognized phenomenon, Mater. Performance 44 (2005) 50–55.
[3] N. Sridhar, K. Price, J. Buckingham, J. Dante, Stress corrosion cracking of carbon steel in ethanol, Corrosion 62 (2006) 687–702.
[4] X. Lou, D. Yang, P.M. Singh, Effect of ethanol chemistry on stress corrosion cracking of carbon steel in fuel-grade ethanol, Corrosion 65 (2009) 785–797.
[5] X. Lou, D. Yang, P.M. Singh, Film breakdown and anodic dissolution during stress corrosion cracking of carbon steel in bioethanol, J. Electrochem. Soc. 157 (2010) C86–C94.
[7] F. Gui, N. Sridhar, J.A. Beavers, Localized corrosion of carbon steel and its implications on the mechanism and inhibition of stress corrosion cracking in fuel-grade ethanol, Corrosion 66 (2010).
[8] J.A. Beavers, F. Gui, N. Sridhar, Effects of environmental and metallurgical factors on the stress corrosion cracking of carbon steel in fuel-grade ethanol, Corrosion 67 (2011).
[9] L.R. Goodman, P.M. Singh, Repassivation behavior of X65 pipeline steel in fuel grade ethanol and its implications for the stress corrosion cracking mechanism, Corros. Sci. 65 (2012) 238–248.
[10] X. Lou, P.M. Singh, Phase angle analysis for stress corrosion cracking of carbon steel in fuel-grade ethanol: experiments and simulation, Electrochim. Acta 56 (2011) 1835–1847.
[11] L. Cao, Corrosion and Stress Corrosion Cracking of Carbon Steel in Simulated Fuel Grade Ethanol, Ohio State University, 2012.
[12] R.C. Newman, Review and hypothesis for the stress corrosion mechanism of carbon steel in alcohols, Corrosion 64 (2008) 819–823.
[13] ASTM-D-4806-06c, Annual Book of ASTM Standards, ASTM International, West Conshohocken, PA, USA, 2006.

(IF = Instruction Fetch, ID = Instruction Decode, EX = Execute, MEM = Memory access, WB = Register write back). In the fourth clock cycle (the green column), the earliest instruction is in MEM stage, and the latest instruction has not yet entered the pipeline. In computer science, instruction pipelining is a technique for implementing instruction-level parallelism within a single processor. Pipelining attempts to keep every part of the processor busy with some instruction by dividing incoming formation of quenched X65 micro-alloyed pipeline steel. Z X Qiao1,*, H X Mi1, J Huo2, Y B Wan1 and X Chen1. 1School of Mechanical Engineering, Tianjin University of Commerce, Tianjin 300134Â API-5L X65 in solution shows a faster crack extension than MAS-in solution. It is found that Jstr (fracture toughness derived from stretch zone geometry) obtained for the two steels exhibits a similar trend with Ji (initiation fracture toughness) which is obtained at the departure of the blunting line on their J-R curves and thus suitable for representing the initiation toughness of the two steels in solution. For bioethanol production from cassava rhizome only the conjugated effect of water, energy co-production were tested (CR-A) (see Table 3). After screening (step 6.2), HC-C and CR-A were the retrofit options chosen with respect to bioethanol production from hardwood chips and cassava rhizome, respectively.Â Other models can also include the effect of the medium temperature on kinetic parameters, which brings additional information for better process description. Models based on neural networks have also been used to describe the fermentation process (Mantovanelli et al., 2007).Â Bioethanol production by yeasts is widely used for biodegradation of potato. However, yeasts cannot ferment starch directly, and a two-step enzymatic reaction to glucose is necessary.